Poly(vinyl chloride)-hyperbranched polyamidoamine ultrafiltration membranes with antifouling and antibiofouling properties

Berta Díez[1], Arcadio Sotto[2,*], Antonio Martín[3], Jesús Arsuaga[3], Roberto Rosal[1,*]

[1] Department of Chemical Engineering, University of Alcalá, E-28871 Alcalá de Henares, Madrid, Spain
[2] Department of Science Education, Rey Juan Carlos University. Camino del Molino, Fuenlabrada. Madrid, Spain.
[3] School of Experimental Science and Technology, ESCET, Rey Juan Carlos University, E-28933 Móstoles, Madrid, Spain

[*] Corresponding authors: arcadio.sotto@urjc.es; roberto.rosal@uah.es

Abstract

Poly(vinyl chloride) (PVC) ultrafiltration membranes with improved antifouling and antibiofouling properties were prepared by non-solvent induced phase inversion using a hyperbranched polyamidoamine as additive. PVC reacted into the casting solution with the commercial polyamidoamine nanomaterial Helux-3316 by means of a nucleophilic substitution reaction. The composition of neat and functionalized membranes was studied by ATR-FTIR and elemental composition. Amino groups were tracked using the fluorescent dye fluorescamine. Surface ζ-potential and water contact angles were used to measure surface charge and hydrophilicity of tested membranes. The incorporation of amino groups increased membrane hydrophilicity and surface porosity, which resulted in enhanced permeability. Functionalized membranes displayed antifouling behaviour revealed upon filtering BSA solutions and lower irreversible fouling than PVC membranes. The attachment of Helux moieties to PVC yielded membranes with antibiofouling functionality explained by the interaction of positively charged Helux moieties with the negatively charged cell envelopes. Growth reduction for cells attached to the membrane surface during filtration reached up to 1-log for the gram-positive bacterium *S. aureus*. This investigation revealed that the incorporation of the hyperbranched nanomaterial in concentrations in the order of 1 wt% in the casting solution provides significant benefits to membrane performance, in terms of permeability and antifouling potential.

Keywords: Poly(vinyl chloride); hyperbranched nanomaterials; ultrafiltration membranes; fouling; biofouling.

Introduction

Membrane processes are key technologies for sustainable industrial development. They are able provide efficient separations with the potential to replace other conventional and energy-intensive techniques. Membrane efficiency is based on the absence of phase changes as well and on the possibility, they offer to reduce energy consumption by recycling product and waste streams [1]. Ultrafiltration is a pressure-driven separation widely used for the separation of particulate matter and macromolecules from soluble compounds and for the treatment of stable oil-in-water emulsions. Ultrafiltration is widely used as desalination pre-treatment, and for wastewater reclamation, either from domestic or industrial effluents [2]. Increased regulatory pressure intensifies the use of water filtration operations, and, therefore, the demand for membranes is steadily increasing even despite certain recent slowdown due to the lower world economic growth. Technological advancements in membrane technologies are expected to lead to additional cost reductions and market growths. One of the main drawbacks of membranes in water treatment operations is flux decline due to the interaction with organic or inorganic substances or with growing microbial cells.

Inorganic fouling is the consequence of the accumulation of particles on membrane surface and inside the pores, eventually creating a cake layer. Organic fouling is due to the adsorption of natural organic matter on external and internal membrane surfaces, eventually blocking or constricting pores. Natural organic matter, particularly extracellular polymeric substances, and soluble macromolecules have been reported as primary organic foulants [3]. Biofouling refers to the growth of microbial cells on membrane surface where they adhere and form biofilms. The interaction between membranes and bacteria starts by non-specific adsorption followed by adherence mediated by the exopolysaccharides (EPS) segregated by bacterial cells during biofilm forming process [4]. Biofilms are complex biological communities that evolved to protect bacteria and, once formed, are very difficult to remove, therefore leading to permanent flux declines [5].

The usual strategy to control fouling and biofouling in ultrafiltration processes is back-washing with cleaning

agents or disinfectants. Chlorinated water is customary used to inactivate microorganisms on chlorine-resistant membranes [6]. Besides, backwashing is needed to remove EPS binding microorganisms [7]. Many authors reported new types of antifouling or antibacterial membranes based on several principles. The use of metal nanoparticles has been frequently proposed due to the toxic effect of many metals to bacterial cells. Copper, silver and other metals, either by direct contact or mediated by the release of different ions have been shown to induce oxidative stress, membrane disruption, and interference with bacterial enzymatic activities [8]. Accordingly, metal nanomaterials have been incorporated to the polymeric matrix to prepare hybrid antifouling ultrafiltration membranes [9, 10].

Another strategy against flux decline is the use of fillers enhancing membrane hydrophilicity [11]. The incorporation of hydrophilic nanofillers in the polymer casting solution was shown to increase permeate flux in mixed matrix ultrafiltration membranes [12]. Zeolites, mesoporous silica and related materials have been shown to modify pore size and interconnectivity as well as surface hydrophilicity achieving increased membrane permeability and durability. Improved antifouling activity has been reported in silica particles upon functionalization with positively and negatively charged amino and carboxylic moieties also accompanied by hydrophilicity enhancement and changes in pore structure [13]. The incorporation of nanoparticles into polymeric membranes has some disadvantages. One is the difficulty to create homogeneous membranes with good particle dispersion due to the tendency of nanoparticles to aggregate. Besides, the possible release of nanomaterials into the environment poses additional concerns.

The integration of anti-fouling properties to hydrophobic membranes has also been performed by hydrophilic polymeric modifiers, the effect of which is to increase flux by creating more water-compatible surfaces or to enhance pore formation [14]. Hydrophilic substances moieties like polyethylene glycol (PEG) or polyvinylpyrrolidone (PVP) are usually incorporated to different type of hydrophobic membrane-forming polymers by blending [15]. Additionally, the use of surface modifying macromolecules, based on active additives able to migrate to the surface specifically changing surface chemistry, has been explored. Kim et al. prepared urethane prepolymer with different end-capping agents generally resulting in narrower pore size distributions and higher pore density membranes [16, 17]. A similar approach, based on incorporating hydrophilic surface modifiers with silver salts, allowed creating anti-biofouling membranes [18].

Helux-3316 is a hyperbranched polymeric nanomaterial that consists of a polyamide backbone with terminal primary amine end-groups together with a lower amount of carboxylic acids. Hyperbranched polymers are a class of dendritic materials, the family also comprising dendrimers, created from a central core upon random branching. Unlike dendrimers, hyperbranched polymers are irregularly shaped and their relatively facile, one-step synthesis make them cheaper [19]. Due to their relatively low cost, hyperbranched polymers have large-volume applications. Lupasol® is a hyperbranched poly(ethyleneimine) used as crosslinker of epoxy resins [20]. Boltorn® hyperbranched materials are in use as ink component [21]. Chemically, hyperbranched polymers are characterized by having a large number of reactive groups, higher solubility than similar molecules of comparable weight and low viscosity, which grant a variety of uses in diverse fields [22].

In this work, we used the hyperbranched polyamidoamine Helux-3316 manufactured by Polymer Factory (Sweden) to functionalize poly(vinyl chloride) ultrafiltration membranes. The approach followed was to chemically bind the polyamidoamine nanomaterial to poly(vinyl chloride) backbone by means of a nucleophilic substitution reaction of chlorine atoms. The concentration of the hyperbranched nanomaterial was in the order of 1 wt% in the casting solution. The new type of modified ultrafiltration membranes has been studied in terms of permeability, organic fouling and antibiofouling/antimicrobial functionality.

2. Materials and methods

2.1. Materials

Hyperbranched polyamidoamine (Helux-3316) was supplied from Polymer Factory (Stockholm, Sweden). Helux-3316 contains primary amines end-groups with a theoretical molecular weight of 5108 g/mol. The chemical structure of Helux-3316 is shown in Fig. S1 (Supplementary Material, SM). Poly(vinyl chloride) (PVC, average molecular weight 43 kDa) and polyvinylpyrrolidone (PVP, average molecular weight 40 kDa) were acquired from Sigma-Aldrich. N, N-dimethylacetamide (DMAc, 99,9%), dimethyl sulfoxide (DMSO, 99,9%), glutaraldehyde solution (25% in H2O), sodium cacodylate, bovine serum albumin (BSA) and fluorescamine were obtained from Sigma-Aldrich. Ultrapure water with a specific resistance of 18.2 MΩ cm -1 was produced by a Direct-Q 5 Ultrapure Water Systems (Millipore, USA). Live/Dead BacLight kits were acquired from Invitrogen (Thermo-Fisher, Waltham, MA). The components of culture media were purchased from Laboratorios Conda (Spain).

2.2. Membrane preparation

Membranes were prepared using the non-solvent induced phase inversion method from a casting solution containing 15 wt% PVC as base material and 5 wt% PVP in DMAc. PVP was used as pore forming additive due to its role of polymer surfactant during gelation process, which is known to result in higher porosity and permeation fluxes [23]. For Helux-PVC membranes,

Helux-3316 was added into the casting solution, and heated at 60 ºC for 10 h under stirring.

After complete dissolution, or after heating in the case of Helux-PVC membranes, the solution was kept still for at least 12 h at room temperature in order to remove any air bubbles present. Afterwards, the solution was cast to 200 µm thickness films onto a glass plate using an automatic film applicator AB3120 (TQC, The Netherlands) and immediately immersed into a water coagulation bath where the solvent (DMAc) and the non-solvent (water) exchanged. Finally, membranes were washed and stored in a new container containing fresh distilled water.

Some specimens were prepared without PVP for comparison purposes and for allowing the assessment of Helux-PVC coupling by tracking their nitrogen content without the interference of nitrogen from PVP. Table 1 summarizes the concentrations and the nomenclature used in what follows.

Table 1. Composition of casting solutions.

Membrane	PVC (% w/w)	PVP (% w/w)	Helux (% w/w)
PVC	15	-	-
PVC-PVP	15	5	-
PVC-PVP-H [0.8]	15	5	0.8
PVC-PVP-H [1.6]	15	5	1.6
PVC-H [0.8]	15	-	0.8
PVC-H [1.6]	15	-	1.6

2.3 Membrane characterization

The morphology of membranes was studied by observing their cross-section under scanning electron microscopy (SEM, Zeiss DSM-950 apparatus operating at 25 kV). Prior to observation, the membranes were frozen in liquid nitrogen and covered with gold. The surface pore size distribution of membranes was assessed by Field Emission Gun Scanning Electron Microscopy (FEG-SEM, FEI, the Netherlands) using membrane specimens sputtered with platinum (5 nm thickness). For microscopic pore size measurements, four samples of each type of membrane were analysed. Statistical pore size distribution and membrane surface porosity were calculated based on FEG-SEM images processed by means of a threshold filter that allowed identifying membrane pores as darker points on the membrane surface. The composition of PVC and Helux-PVC membranes was analysed by Attenuated total reflectance Fourier transform infrared (ATR-FTIR) spectra using a Thermo-Scientific Nicolet iS10 apparatus with a Smart iTR-Diamond ATR module. Elemental composition analyses were performed using a LECO CHNS-932 Analyzer.

Surface ζ-potential was determined by electrophoretic light scattering using a Zetasizer Nano apparatus (ZEN1020) from Malvern (Malvern Instruments, UK). Surface zeta potential measurement consisted of holding a rectangular section of each membrane between two electrodes using araldite adhesive. The sample was then immersed into an appropriate aqueous solution containing 10 mM KCl (pH 7.0) and 0.5 % (w/w) of polyacrylic acid (450 kDa) acting as a tracer. The electrophoresis mobility of the tracer was measured at six different distances from the sample surface. Measurements were conducted at room temperature (25 ºC). Static water contact angles (WCA) were studied by the sessile drop technique using a Krüss DSA25 equipment. Surface ζ-potential and WCA were calculated using at least four replicates with different specimens. All measurements were performed at room temperature.

In order to assess the grafting of amino groups from Helux to PVC in Helux-PVC membranes, we used fluorescamine as probe for confocal microscopy imaging. Fluorescamine is a non-fluorescent compound that reacts with primary amines forming a stable and highly fluorescent product. A fresh stock solution of fluorescamine (3 mg/mL in acetone) was prepared, extended onto membrane surface, and incubated for 15 min at room temperature. Subsequently, the membranes were washed and visualized using a confocal microscope with fluorescence module (TCS-SP5 Leica Microsystems) at excitation/emission wavelengths of 365 nm/470 nm respectively. PVC membranes without any source of nitrogen in their structure were also treated with fluorescamine as a negative control. The stability of Hellux-3316 as a source of nitrogen in the aminated membranes was tracked, after 48 h of water filtration at 2 bars transmembrane pressure (TMP).

2.4 Filtration and fouling assays

Filtration assays were conducted using a crossflow stainless-steel module connected to a 2 L volume tank kept at 25 ºC. The effective area of the membrane samples was 20 cm^2 (40 mm x 50 mm). Pure water flux (J_w) was measured at different transmembrane pressures (TMP) in the 1 to 4 bar range. Prior to permeability tests, membranes were compacted for about 2 hours at 4 bars with deionized water in order to obtain reproducible and representative flux measurements. Flux measurements were performed at transmembrane pressure (TMP) 2 bar. Four specimens of each membrane were tested. Pure water flux (J_w^i) was calculated using following equation:

$$J_w^i = \frac{V}{A\,\Delta t} \quad (1)$$

Where V (L) is the volume of permeate collected, A (m^2) is the membrane effective area and Δt (h) is the operation time.

Membrane fouling was studied using BSA as model of organic foulant. For it, BSA was dissolved in 0.1 M phosphate-buffered physiological saline (PBS) at a concentration of 1.0 g/L, pH 7.2. Once pure water flux was measured in permeation tests, water was replaced

by the BSA solution and flux allowed to stabilize. Then, BSA solution was kept flowing for 3 h, after which the flux of fouled membranes was recorded (J_p, before cleaning specimens). Then, membranes were rinsed with distilled water and pure water flux of cleaned specimens (J_w^f) was recorded again. At least five filtration experiments were carried out for each polymer composition until reproducible values were obtained. All values were recorded at 2 bat TMP.

The average surface pore radius of membranes, rm, was also estimated using was the Guerout–Elford–Ferry equation:

$$r_m = \sqrt{\frac{(2.9-1.75\,\varepsilon)\,8\,J\,L\,\eta}{\varepsilon\,\Delta P}} \quad (2)$$

Where η is the viscosity of water (8.9 × 10−4 Pa s), and ε membrane porosity determined by weighing wet and dry membranes. The obtained radius is considered an average of all pores creating permeate flow.

Flux recovery ratio (FRR) was calculated as follows:

$$\text{Flux recovery ratio (\%)} = \frac{J_w^f}{J_w^i} \times 100 \quad (3)$$

Flux loss was assessed in terms of total, reversible and irreversible fouling ratio (TFR, RFR and IFR, respectively) as indicated in the following equations:

$$\text{Total fouling ratio (\%)} = \left(1 - \frac{J_p}{J_w^i}\right) \times 100 \quad (4)$$

$$\text{Reversible fouling ratio (\%)} = \left(\frac{J_w^f - J_p}{J_w^i}\right) \times 100 \quad (5)$$

$$\text{Irreversible fouling ratio (\%)} = \left(1 - \frac{J_w^f}{J_w^i}\right) \times 100 \quad (6)$$

Rejection efficiency (*R*) was calculated according to the following equation:

$$R(\%) = \left(1 - \frac{C_p}{C_f}\right) \times 100 \quad (7)$$

Where C_p and C_f represent the concentration of BSA in permeate and feed solutions, respectively. The concentration of foulant was recorded by UV spectrophotometry at 280 nm.

2.5 Antibiofouling assays

The antimicrobial activity of prepared membranes was tested using two different bacterial strains, *S. aureus* (CECT 240, strain designation ATCC 6538P) and *E. coli* (CECT 516, strain designation ATCC 8739), Gram-positive and gram-negative respectively. The microorganisms were maintained in glycerol at -80 ºC until use. Nutrient broth culture medium (NB) was used to reactivate bacterial growth using a pH 6.8–7.0, after which bacterial cultures were kept at 36 ºC under constant stirring (250 rpm). Bacterial growth for initial cultures was monitored by tracking optical density (OD) at 600 nm.

The antibiofouling behaviour of membranes was estimated by counting the CFU (colony forming units) according to the standard procedure described in the ISO 22196, with minor modifications. Cultures with an initial bacterial concentration of 106 cells/mL were prepared and inoculated in sterile 24-wells microplates, using a NB medium diluted 500-fold. Membranes were sterilized and then soaked in bacterial cultures, maintaining them for 20 h at 36 ºC. The amount of inoculum used was 0.3 mL/mg of membrane. After incubation, the bacterial cells present in the culture medium and cells detached from membranes were quantified by counting colony-forming units (CFU). For that, 10-fold serial dilutions were performed in PBS, then 10 µL of each dilution was spot-plated on solid agar and incubated at 36 ºC for 24 h before counting colonies. Adhered cells were obtained using soybean casein digest broth with lecithin and polyoxyethylene sorbitan monooleate, following the guideline described in ISO 22196. Prior to it, membranes were washed with PBS for 30 min in an orbital shaker to remove the non-adhered cells. Each sample was measured in triplicate in three independent runs.

Colonized membranes were visualized using SEM images. Membranes were incubated for 20 h with bacterial cultures of initially 10^6 cells/mL of *E. coli* or *S. aureus*. Afterwards, membranes were cleaned with distilled water, fixed using glutaraldehyde (5% v/v) in sodium cacodylate (0.2 M) and dehydrated using different concentrations of ethanol (25%-50%-70-90-100 % v/v) and acetone (100 % v/v). SEM micrographs were obtained in a ZEISS DSM-950 instrument operating at 25 kV.

Bacterial viability was examined by means of the Live/Dead BacLight Bacterial Viability kit. This method uses two different fluorescent nucleic acid stains, SYTO 9 and propidium iodide (PI) which differentiate viable and non-viable cells, respectively. It is based in their ability to penetrate healthy bacterial cells. SYTO 9 can penetrate intact and damaged membranes, marking cells in green. In contrast, propidium iodide is only internalized by membrane-damaged cells, marking cells in red. The images were obtained by the confocal laser microscopy (LEICA TCS-SP5) using an excitation/emission wavelength of 472 nm/580 nm respectively.

3. Results and discussion

The reactivity of chloride atoms in the poly(vinyl)chloride main chains allows chemical modification without affecting the polymer backbone by means of nucleophilic substitution reactions [24, 25]. In this study, the hyperbranched polyamidoamine Helux-3316 was used as a nucleophile for the amination reaction of PVC chains by means of the SN2 reaction.

Helux substituted chlorine atoms from PVC chains giving rise to aminated-PVC chains in DMAc solution. Fig. S2 (SM) shows a schematic representation of the production process of Helux-PVC ultrafiltration membranes. Fig. 1 shows cross-sectional SEM images of PVC and Helux-PVC membranes displaying asymmetric structure with dense skin layer on top of a finger-like porous sublayer.

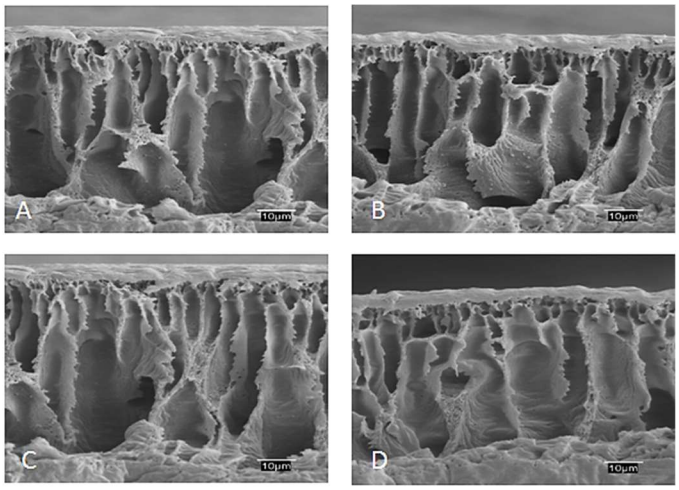

Figure 1. SEM cross-sectional images of neat PVC (A), PVC-PVP (B), PVC-PVP-H [0.8] (C) and PVC-PVP-H [1.6] (D) membranes.

The formation of larger finger-like pores structures is clear in modified PVC membranes. It could be explained by the faster diffusion exchange between solvent and non-solvent during the phase inversion process due to the action of hydrophilic components into the polymer solution. Morphological changes include improved pore interconnectivity, which enhances water permeation [10]. Fig. S3 (SM) shows images of membranes prepared without PVP. Fig. S4 shows FEG-SEM images of membranes prepared with and without Helux. Surface pore size distribution was obtained by processing images using a threshold filter. The results showed that the incorporation of Helux resulted in a significant increase in the number of pores, but not their diameter, which was (modal value) in the 20-30 nm range both for PVC-C and Helux-modified PVC-PVP-H [1.6] membranes. Based on Guerout–Elford–Ferry equation, the incorporation of Helux slightly increased average por diameter from 35.5 ± 1.0 nm for PVC-C to 47.1 ± 0.6 nm in PVC-PVP-H [1.6] specimens, which was probably due to the presence of some proportion of larger pores in Helux-functionalized membranes. The evaluation of porosity based on FEG-SEM images indicated 1.05 % of surface porosity for PVC-C and 1.41 for PVC-PVP-H [1.6], representing a 34% increase.

FTIR spectra confirmed the presence of the main functional groups of polymers on membranes (Fig. 2). Fig. 2A displays the FTIR spectra of neat PVC, PVP-PVC and Helux-PVC membranes showing the characteristic peaks of the polymers. The band at 2890–2958 cm^{-1} corresponded to C–H stretching mode. CH_2 deformation appeared at 1320 cm^{-1}, out of plane angular deformation of CH at 1230 cm^{-1}, trans CH wagging at 960 cm^{-1}, C-Cl stretching at 845 cm^{-1}, and cis CH wagging at 650 cm^{-1} [26]. The spectra of PVP-doped membranes also revealed the characteristic bands of PVP. Besides the absorptions corresponding to hydrocarbon backbone, the peat at 1660 cm^{-1} was attributed to the stretching vibration of the carbonyl groups, C=O, from the pyrrolidone ring [27, 28]. The presence of Helux in Helux-PVC membranes can be confirmed by the FTIR spectra of Helux-PVC membranes from the shoulder at 3240 cm^{-1} corresponding to N-H stretching of amides, the C-H stretching signal in the 2800-2900 cm^{-1}, and the peak at 1528 cm^{-1}, which corresponded to the N-H bend in amides and amines. In order to clarify the presence of aminated groups, some additional specimens were prepared without PVP, namely PVC- H [0.8 and 1.6]. In this case, membranes showed a new peak at 1648 cm^{-1} corresponding to the amide C=O stretch, consistent with the incorporation of Helux functional groups into the structure of PVC membranes. Their spectra together with that of pure Helux are shown in Fig. 2B. Coincidences with Helux peaks in FTIR spectra are indicated with arrows.

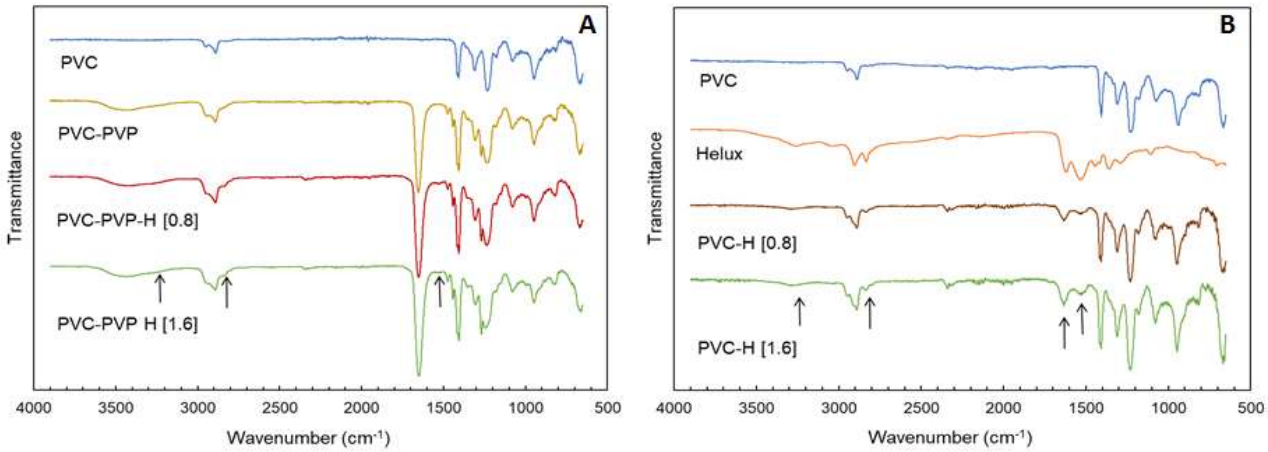

Figure 2. A) ATR-FTIR spectra of PVC, PVC-PVP, and Helux-PVC membranes PVC-PVP-H [0.8] and PVC-PVP-H [1.6]. B) FTIR spectra of Helux, and Helux-PVC membranes prepared without PVP: PVC-H [0.8] and PVC-H [1.6].

Surface ζ-potential was used to characterize membrane surface charge [29]. The surface ζ-potential at pH 7.0 of representative specimens are shown in Table 2. Neat PVC membranes displayed a zeta potential value of -34.1 ± 1.3 mV. Negative surface charge in polymeric membranes is a usual finding, attributed to the preferential adsorption of negative ions [30]. As result of Helux addition (a compound bearing 10 primary amino groups), the ζ-potential values of Helux-PVC membranes increased to -24.0 ± 2.6 mV and -14.0 ± 2.5 mV for Helux concentration in the casting solution of 0.8 % and 1.6 %, respectively. The pK_a values of aliphatic primary and secondary amines is ~10 and, therefore, they are positively charged at neutral pH [31]. The reduction of the negative charge of PVC upon amination indicated that the introduction of positively charged $-NH_3^+$ or $-NH_2^+$- groups partly compensated PVC negative charge, leading to less negative ζ-potential values [28].

The hydrophilicity of PVC and Helux-PVC membranes was studied by measuring the water contact angles (WCA) created between water drop and membrane surface. The results obtained are also represented in Table 2. The incorporation of Helux resulted in slightly decreased water contact angles values, compared to neat PVC membranes. The effect was most probably due to the presence of charged amines that stabilise intermolecular hydrogen bonds with water molecules, leading to higher hydrophilicity for Helux-PVC membranes.

Table 2. Membranes properties

Membranes	Surface ζ-potential (mV)[a]	WCA (º)	Flux (LMH)[b]	Rejection (%)[b]
PVC-C	-34.1 ± 1.3	78.4 ± 2.7	89.5 ± 2.7	89.2 ± 0.8
PVC-PVP	-31.7 ± 1.3	73.4 ± 1.7	114.4 ± 1.3	88.1 ± 1.1
PVC-PVP-H[0.8]	-24.0 ± 2.6	69.9 ± 1.6	131.2 ± 2.0	89.6 ± 1.6
PVC-PVP-H[1.6]	-14.0 ± 2.5	65.9 ± 2.1	149.4 ± 0.6	87.6 ± 1.7
PVC.H [0.8]	-26.4 ± 1.3	72.3 ± 2.6	128.2 ± 1.0	88.9 ± 0.6
PVC.H [1.6]	-18.3 ± 1.1	69.3 ± 1.9	137.6 ± 1.3	87.9 ± 1.4
Helux-3316 pure	+8.9 ± 2.1[c]	-	-	-

[a] Surface zeta potential was measured at pH 7.0
[b] Operation at 2 bar TMP
[c] ζ-potential in aqueous dispersion (Milli-Q ultrapure water)

Table 3: Fouling parameters of PVC and Helux-functionalized membranes

Membrane	TFR (%)	RFR (%)	IFR (%)	FRR (%)
PVC	37.8 ± 1.0	17.9 ± 1.3	19.9 ± 0.3	77.7 ± 3.6
PVC-PVP	33.3 ± 2.1	17.1 ± 0.7	16.2 ± 1.3	83.0 ± 0.5
PVP-PVP-H [0.8]	28.6 ± 1.2	16.7 ± 2.4	11.9 ± 1.1	88.1 ± 1.1
PVP-PVP-H [1.6]	32.5 ± 2.0	18.5 ± 3.5	14.8 ± 2.4	84.6 ± 3.2

The incorporation of amino groups into PVC membranes was visually assessed using the fluorescent dye fluorescamine, which is a molecule that interacts with primary amines, forming stable Helux-fluorescamine conjugates [32]. Fig. S5 (SM) shows confocal images of neat PVC and Helux-PVC membranes after exposure to fluorescamine dye. Helux-PVC membranes revealed a blue fluorescent colour distributed across their surface, indicating the presence of aminated groups. The intensity of Helux-fluorescamine conjugate increased with increasing concentration of Helux in the casting solution. PVC membranes used as a negative control were treated with the same concentration of fluorescamine and showed absence of any blue fluorescence.

Elemental analysis was used to quantify the amount of Helux-3316 grafted into PVC membranes. The percentage of nitrogen was measured in PVC-H [0.8] and PVC-H [1.6] membranes, which contain Helux as the only source of nitrogen. Membrane specimens containing PVP were not analysed due to the interference of nitrogen from PVP. Fig. 3 **s**hows that as the concentration of Helux increased from 0.8 % to 1.6 % in the casting solution, the percentage of nitrogen included in membranes increased from 1.1 ± 0.3 % to 2.2 % ± 0.7, respectively. These data support the assumption that the Helux used in casting solutions became effectively incorporated into the final membranes. In order to assess the stability of Helux included in membranes, a series of filtration assays were performed at 2 bar TMP for 48 h. The results of nitrogen measurements showed that Helux did not significantly leak out from membranes during operation, indicating stable functionalization.

Pure water flux for neat PVC, PVC-PVP and Helux-PVC membranes is indicated in Table 2. The results showed that permeation rate increased from 89.4 ± 2.7 LMH obtained for neat PVC membranes up to 114.4 ±

1.3 and 149.4 ± 0.6 LMH for PVC-PVP membranes and Helux-functionalized PVC membranes, respectively. It is a known fact that hydrophilic additives such as PVP or polyethylene glycol are excellent pore-forming agents [33]. Such additives enhance phase-separation during membrane fabrication and contribute to the increase the number of membrane pores, which results in higher membrane permeability [13]. The increase in the number of pores is the most probable reason for the observed flux increase in view of the results obtained from FEG-SEM images about pore size distribution. The higher hydrophilicity of Helux-PVC membranes is also expected to increase water permeability and to mitigate the membrane surface fouling.

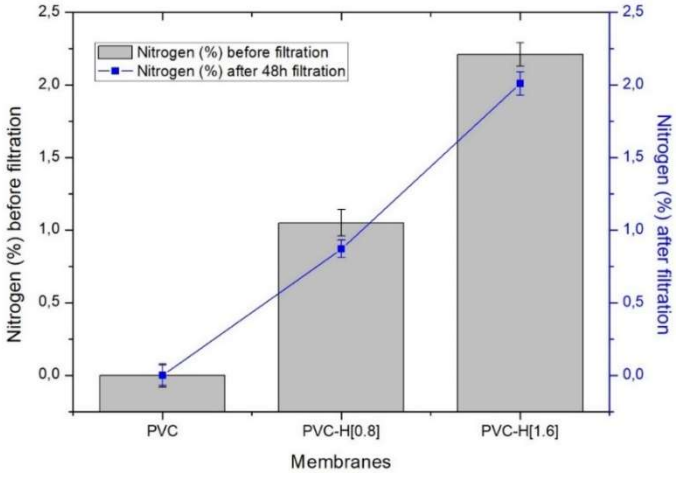

Figure 3. Percentage of nitrogen in PVC and Helux-PVC membranes before and after 48h of water filtration at 2 bar TMP. Error bars represent standard deviation.

The antifouling performance of PVC and Helux-PVC membranes was studied using BSA as a protein model for organic fouling. The decrease in flux due to the adsorption and deposition of organic fouling was measured by recording water flux before and after BSA filtration. BSA solution (1g/L) was kept flowing for 3 h at 2 bar TMP after stabilization, and pure water flux was recorded as indicated before. Fouling parameters: Total Fouling Ratio (TFR), Reversible Fouling Ratio (RFT), Irreversible Fouling Ratio (IFR) and flux recovery ratio (FFR) were calculated as shown in equations 3-6. The results are summarized in Table 3.

The effect of the modification proposed on the antifouling character of prepared membranes was clear in all of cases. Expressed in terms of permeation rate, we obtained 55.7 ± 2.2 LMH for PVC-C membranes and 100.8 ± 2.4 LMH for PVC-PVP-H [1.6], which represented 80% increase after 3 h filtering 1 g/L BSA solution. TFR decreased from 38 % for neat PVC membranes up to 29-33 % for PVC-PVP and Helux-PVC membranes. The results can be attributed to their higher hydrophilicity due to the presence of PVP or Helux, indicating better antifouling properties. Total flux loss can be produced by reversible or irreversible fouling. Irreversible fouling was higher in neat PVC membranes (19.9 %). It is known that hydrophobic membranes are prone to suffer the adsorption of proteins due to hydrophobic interactions, blocking membrane pores and inducing the formation of a surface cake layer [34]. Irreversible fouling is only partially removed by chemical cleaning, which is associated to membrane damage, thereby reducing membrane life [35]. Both TFR and IFR decreased in Helux-functionalized membranes, a fact that was attributed to their higher hydrophilicity. A possible reason for not observing significantly lower RFR might be the electrostatic interaction between the positively charged amino groups of Helux-PVC membranes and negative charged BSA [28]. BSA rejection tests carried out by measuring the protein concentration in permeates allowed calculating rejection efficiency, which is shown for all tested specimens in Table 2. Similar retention properties were obtained for PVC and Helux-functionalized membranes, with only a slight non-significant reduction in membranes containing PVP, which could eventually be related to pore size increase during membrane preparation.

The microorganisms tested in this work as biofoulants were the gram-negative *E. coli* and the gram-positive *S. aureus*, strains commonly used as representative for both types of microorganisms in antimicrobial activity tests. Figure S6 (SM) shows the number of viable bacteria, express as a CFU (colony forming units) present in the liquid medium (NB 1/500) kept in contact for 20 h at 36 ºC with different membranes specimens. The results showed that the growth of *E. coli* and *S. aureus* decreased for Helux-functionalized specimens, most probably due to the presence of positively charged amines on their surface. Anti-biofouling was measured by counting cells adhered to the membrane surface after detaching them using the procedure given in the ISO 22196 and outlined before. Fig. 4 showed that after 20 h in contact with the membranes at 36 ºC, the bacterial cells responsible for biofilm formation, were considerably reduced in Helux-PVC membranes. About 1-log reduction was observed for *S. aureus* growth, with a somewhat lower effect for *E. coli*. The differences between both strains are due to evolutionary reasons that provided gram-negative bacteria additional protection. A higher resistance of gram-negative bacteria to antimicrobials is a usual finding, usually attributed to their different structure as explained below.

The antimicrobial efficiency of Helux-PVC membranes can be attributed to the presence of primary or secondary amines in functionalized membranes. Helux molecules displays polycationic character at physiological pH, due to its protonated amine groups as revealed by its ζ-potential of +8.9 ± 2.1 mV. Table 2 showed that surface zeta potential became less negative upon Helux functionalization of PVC membranes that partially neutralize the negative charge of PVC. Overall, membrane surface should contain positively

charged domains associated to Helux moieties, which are susceptible to interact with the negatively charged bacterial wall therefore contributing to the disruption of membrane structures [36].

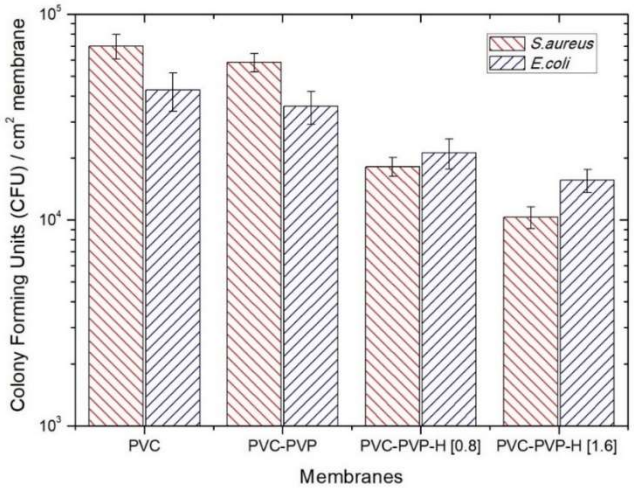

Figure 4. Viable microorganism detached from membranes specimens exposed to *S. aureus* and *E. coli* cultures after 20 h at 36 ºC. Errors bars indicate standard deviation.

The external difference between cell wall structures of gram-positive and gram-negative could explain this behaviour. gram-negative bacteria contain a thin cell wall surrounded by two plasma membrane layers, the outer membrane (OM) contains polyanionic lipopolysaccharides (LPS) neutralized by divalent cations, as a Ca^{2+} and Mg^{2+} [36, 37]. Gram-positive bacteria contain a thick cell wall composed by different layers of peptidoglycan and lipoteichoic acids that also requires cationic counterions to stabilize the assembly [38]. Cation-binding sites are essential for maintaining the cell wall structure. However, amino charged groups could interact with divalent cations competing for the electronegative sites on cell membranes [37, 39]. These electrostatic interactions may disrupt cell wall structure leading to increased membrane permeability [40-42]. Although the exact mechanism of action varies between polycations, membrane damage leads to osmotic imbalances and, eventually, cell lysis [43, 44].

The disruption of the cell wall membrane was confirmed by confocal images using Live/Dead assay. This method distinguishes viable and non-viable cells according to cell membrane integrity using two fluorescent stains: propidium iodide and Syto9. Propidium iodide is a nucleophilic dye that only penetrates through the damaged membrane, marking the cells in red. Syto9 marks viable cells in green, indicating non-damaged bacterial cells. Fig. 5 shows PVC and PVC-PVP membranes covered only by green-labelled viable cells. However, Helux-PVC membranes revealed a considerable number of red-marked cells indicating cells with damaged membrane integrity and only a few scattered green-marked viable cells.

The anti-biofouling effect of Helux-PVC membranes was studied using SEM micrographs. Fig. 6 shows that Helux-PVC membranes considerably reduce biofilm

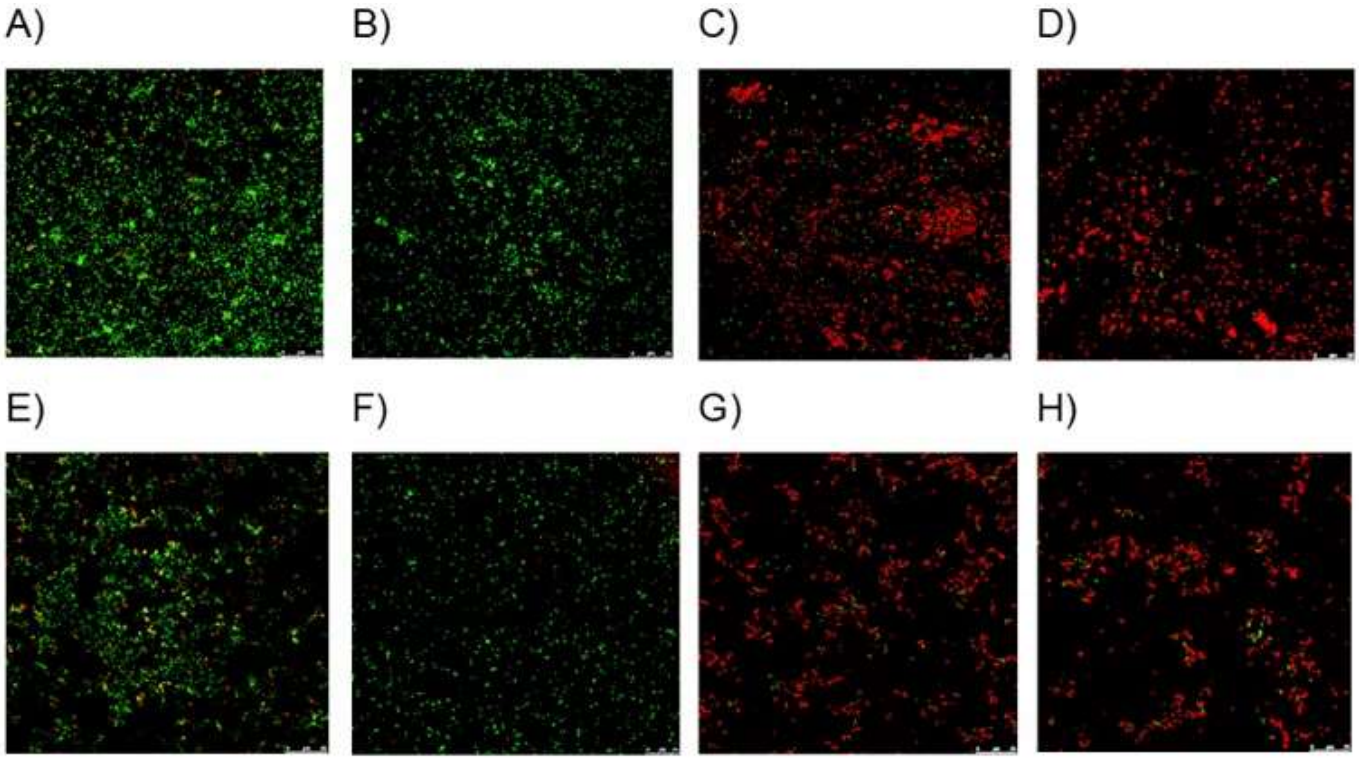

Figure 5. Confocal images of PVC (A, E) PVC-PVP (B, F) PVC-PVP-H [0.8] (C, G) and PVC-PVP-H [1.6] (D, H) membranes after exposure to *S. aureus* (A-D) and *E. coli* (E-H) cultures for 20 h at 36 ºC. Viable bacteria are green marked by viability stain, whereas red dots indicate membrane-damaged cells.

formation. Although certain colonization was observed, the comparison with PVC membranes indicated significantly reduced bacterial growth and biofilm formation. The microbial colonization of PVC-PVP and PVC-PVP-H [0.8] membranes are shown in Fig. S7 (SM). It should be noted that our results refer to flat membranes, but it is expected that anti-biofouling properties will be preserved in other geometries.

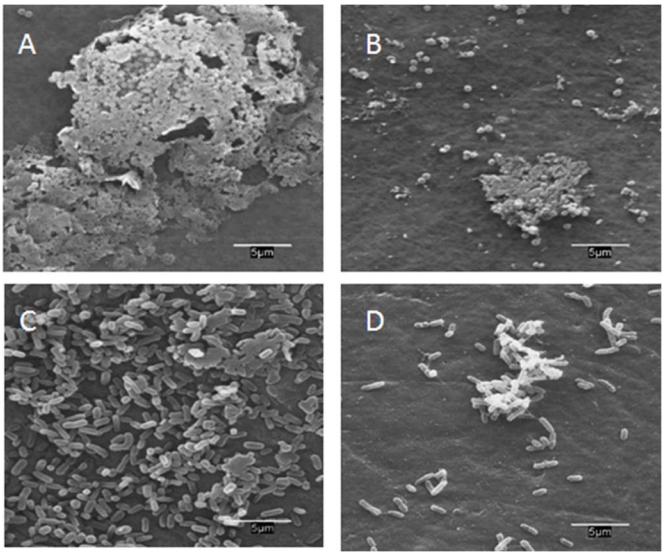

Figure 6. Microbial colonization of *S. aureus* (A-B) and *E. coli* (C-D) after exposure of PVC (A-C) and PVC-PVP-H [1.6] membranes to bacterial cultures for 20 h at 36 ºC.

Combining physicochemical and biological data, we showed that the introduction of the hyperbranched polymeric nanomaterial Helux reduced biofouling by affecting the integrity of microbial cell membranes. Besides, the higher hydrophilicity of Helux-functionalized membranes resulted in higher surface porosity, permeability and decreased irreversible organic fouling. Overall, better hydrodynamic performance and fouling and biofouling resistance would benefit membranes with lower energy consumption, reduced use of chemicals for cleaning procedures and increased membrane life.

5. Conclusions

In this study, new PVC ultrafiltration membranes functionalized with the hyperbranched polymeric nanomaterial Helux-3316 were prepared. The incorporated amine groups were evenly distributed within functionalized membranes and became firmly attached to the polymeric material by covalent bonds. No loss of nitrogen was observed during operation.

The surface ζ potential of Helux-PVC membranes increased from -34.1 ± 1.3 mV in PVC membranes to -14.0 ± 2.5 mV for Helux-loaded specimens, because of positively charged amines at neutral pH. Helux-PVC membranes displayed higher water permeability due to their increased surface porosity compared to PVC membranes and displayed significant resistance against irreversible organic fouling as observed from BSA filtration experiments.

The modified Helux-PVC membranes exhibited clear anti-biofouling character, with up to 1.0-log reduction of bacterial growth on membranes surface. The antimicrobial activity was attributed to the presence of positively charged groups in functionalized membranes, which induced damage of bacterial cell envelopes, eventually rendering cells non-viable.

Acknowledgements

Financial support was provided by the Spanish Ministry of Science, Innovation and Universities (CTM2016-74927-C2-1-R). BD thanks the University of Alcalá for the award of predoctoral grant.

References

[1] M.G. Buonomenna, Membrane processes for a sustainable industrial growth, RSC Adv. 3 (2013) 5694-5740. https://doi.org/10.1039/C2RA22580H.

[2] I. Koyuncu, R. Sengur, T. Turken, S. Guclu, M.E. Pasaoglu, Advances in water treatment by microfiltration, ultrafiltration, and nanofiltration, in: A. Basile, A. Cassano, N.K. Rastogi (Eds.), Advances in Membrane Technologies for Water Treatment: Materials, Processes and Applications, Woodhead Publishing, Elsevier, 2015, pp. 83-128.

[3] N. Subhi, G. Leslie, V. Chen, P. Le-Clech, Organic fouling of ultrafiltration membrane: Detailed characterization by liquid chromatography with organic carbon detector (LC-OCD), Sep. Sci. Technol. 48 (2012) 199-207. https://doi.org/10.1080/01496395.2012.686552.

[4] S. Shao, Y. Wang, D. Shi, X. Zhang, C.Y. Tang, Z. Liu, J. Li, Biofouling in ultrafiltration process for drinking water treatment and its control by chlorinated-water and pure water backwashing, Sci. Total Environ. 644 (2018) 306-314. https://doi.org/10.1016/j.scitotenv.2018.06.220.

[5] C.X. Liu, D.R. Zhang, Y. He, X.S. Zhao, R. Bai, Modification of membrane surface for anti-biofouling performance: Effect of anti-adhesion and anti-bacteria approaches, J. Membr. Sci. 346(1) (2010) 121-130. https://doi.org/10.1016/j.memsci.2009.09.028.

[6] W. Yu, L. Xu, N. Graham, J. Qu, Pre-treatment for ultrafiltration: effect of pre-chlorination on membrane fouling, Sci. Rep. 4 (2014) 6513. https://doi.org/10.1038/srep06513.

[7] T. Nguyen, F.A. Roddick, L. Fan, Biofouling of water treatment membranes: A review of the underlying causes, monitoring techniques and control measures, Membranes 2 (2012) 804-840. https://doi.org/10.3390/membranes2040804.

[8] J.A. Lemire, J.J. Harrison, R.J. Turner, Antimicrobial activity of metals: mechanisms, molecular targets and applications, Nat. Rev. Microbiol. 11 (2013) 371-384. https://doi.org/10.1038/nrmicro3028.

[9] Z. Xu, S. Ye, G. Zhang, W. Li, C. Gao, C. Shen, Q. Meng, Antimicrobial polysulfone blended ultrafiltration membranes prepared with Ag/Cu_2O hybrid nanowires, J. Membr. Sci. 509 (2016) 83-93. https://doi.org/10.1016/j.memsci.2016.02.035.

[10] B. Díez, N. Roldán, A. Martín, A. Sotto, J.A. Perdigón-Melón, J. Arsuaga, R. Rosal, Fouling and biofouling resistance of metal-doped mesostructured silica/polyethersulfone ultrafiltration membranes, J. Membr. Sci. 526 (2017) 252-263. https://doi.org/10.1016/j.memsci.2016.12.051.

[11] L.X. Dong, H.W. Yang, S.T. Liu, X.M. Wang, Y.F. Xie, Fabrication and anti-biofouling properties of alumina and zeolite nanoparticle embedded ultrafiltration membranes, Desalination 365 (2015) 70-78. https://doi.org/10.1016/j.desal.2015.02.023.

[12] J.M. Luque-Alled, A. Abdel-Karim, M. Alberto, S. Leaper, M. Perez-Page, K. Huang, A. Vijayaraghavan, A.S. El-Kalliny, S.M. Holmes, P. Gorgojo, Polyethersulfone membranes: From ultrafiltration to nanofiltration via the incorporation of APTS functionalized-graphene oxide, Sep. Purif. Technol. 230 (2020) 115836. https://doi.org/10.1016/j.seppur.2019.115836.

[13] A. Martín, J.M. Arsuaga, N. Roldán, J. de Abajo, A. Martínez, A. Sotto, Enhanced ultrafiltration PES membranes doped with mesostructured functionalized silica particles, Desalination 357 (2015) 16-25. https://doi.org/10.1016/j.desal.2014.10.046.

[14] G. Arthanareeswaran, D. Mohan, M. Raajenthiren, Preparation, characterization and performance studies of ultrafiltration membranes with polymeric additive, J. Membr. Sci. 350 (2010) 130-138. https://doi.org/10.1016/j.memsci.2009.12.020.

[15] M.Z. Yunos, Z. Harun, H. Basri, A.F. Ismail, Studies on fouling by natural organic matter (NOM) on polysulfone membranes: Effect of polyethylene glycol (PEG), Desalination 333 (2014) 36-44. https://doi.org/10.1016/j.desal.2013.11.019.

[16] Y. Kim, D. Rana, T. Matsuura, W.-J. Chung, Influence of surface modifying macromolecules on the surface properties of poly(ether sulfone) ultra-filtration membranes, J. Membr. Sci. 338 (2009) 84-91. https://doi.org/10.1016/j.memsci.2009.04.017.

[17] Y. Kim, D. Rana, T. Matsuura, W.-J. Chung, K.C. Khulbe, Relationship between surface structure and separation performance of poly(ether sulfone) ultra-filtration membranes blended with surface modifying macromolecules, Sep. Purif. Technol. 72 (2010) 123-132. https://doi.org/10.1016/j.seppur.2010.01.006.

[18] D. Rana, Y. Kim, T. Matsuura, H.A. Arafat, Development of antifouling thin-film-composite membranes for seawater desalination, J. Membr. Sci. 367 (2011) 110-118. https://doi.org/10.1016/j.memsci.2010.10.050.

[19] Y. Zheng, S. Li, Z. Weng, C. Gao, Hyperbranched polymers: advances from synthesis to applications, Chem. Soc. Rev. 44 (2015) 4091-4130. https://doi.org/10.1039/C4CS00528G.

[20] F. Román, P. Colomer, Y. Calventus, J.M. Hutchinson, Study of hyperbranched poly(ethyleneimine) polymers of different molecular weight and their interaction with epoxy resin, Materials 11 (2018) 410. https://doi.org/10.3390/ma11030410.

[21] Z. Żołek-Tryznowska, J. Izdebska, Flexographic printing ink modified with hyperbranched polymers: Boltorn™ P500 and Boltorn™ P1000, Dyes Pigm. 96 (2013) 602-608. https://doi.org/10.1016/j.dyepig.2012.10.003.

[22] C. Gao, D. Yan, H. Frey, Promising dendritic materials: An introduction to hyperbranched polymers, in: D. Yan, C. Gao, H. Frey (Eds.), Hyperbranched Polymers: Synthesis, Properties, and Applications, Wiley, 2011, pp. 1-26.

[23] J. Xu, Z.L. Xu, Poly(vinyl chloride) (PVC) hollow fiber ultrafiltration membranes prepared from PVC/additives/solvent, J. Membr. Sci. 208 (2002) 203-212. https://doi.org/10.1016/S0376-7388(02)00261-2.

[24] T. Kameda, M. Ono, G. Grause, T. Mizoguchi, T. Yoshioka, Chemical modification of poly(vinyl chloride) by nucleophilic substitution, Polym. Degrad. Stab. 94 (2009) 107-112. https://doi.org/10.1016/j.polymdegradstab.2008.10.006.

[25] N. Shaglaeva, R. Sultangareev, E. Zabanova, O. Lebedeva, K. Trofimova, Nucleophilic substitution of chlorine atoms in polyvinyl chloride, Russ. J. Appl. Chem. 81 (2008) 131-134. https://doi.org/10.1134/S1070427208010291.

[26] S. Ramesh, K.H. Leen, K. Kumutha, A.K. Arof, FTIR studies of PVC/PMMA blend based polymer electrolytes, Spectrochim. Acta, Part A 66 (2007) 1237-1242. https://doi.org/10.1016/j.saa.2006.06.012.

[27] Kamaruddin, D. Edikresnha, I. Sriyanti, M.M. Munir, Khairurrijal, Synthesis of polyvinylpyrrolidone (PVP)-green tea extract composite nanostructures using electrohydrodynamic spraying technique, IOP Conf. Ser.: Mater. Sci. Eng. 202 (2017) 012043. https://doi.org/10.1088/1757-899x/202/1/012043.

[28] J. Zhu, Y. Su, X. Zhao, Y. Li, J. Zhao, X. Fan, Z. Jiang, Improved antifouling properties of poly(vinyl chloride) ultrafiltration membranes via surface zwitterionicalization, Ind. Eng. Chem. Res. 53 (2014) 14046-14055. https://doi.org/10.1021/ie5022877.

[29] Y. Qi, L. Zhu, X. Shen, A. Sotto, C. Gao, J. Shen, Polythyleneimine-modified original positive charged nanofiltration membrane: Removal of heavy metal ions and dyes, Sep. Purif. Technol. 222 (2019) 117-124. https://doi.org/10.1016/j.seppur.2019.03.083.

[30] D.B. Burns, A.L. Zydney, Buffer effects on the zeta potential of ultrafiltration membranes, J. Membr. Sci. 172 (2000) 39-48. https://doi.org/10.1016/S0376-7388(00)00315-X.

[31] V.S. Bryantsev, M.S. Diallo, W.A. Goddard, pKa calculations of aliphatic amines, diamines, and aminoamides via density functional theory with a Poisson−Boltzmann continuum solvent model, J. Phys. Chem. A 111 (2007) 4422-4430. https://doi.org/10.1021/jp071040t.

[32] I. Martín-de-Lucía, F. Leganés, F. Fernández-Piñas, R. Rosal, Hyperbranched polymeric nanomaterials impair the freshwater crustacean *Daphnia magna*, Environ. Pollut. 249 (2019) 581-588. https://doi.org/10.1016/j.envpol.2019.03.078.

[33] P.T.P. Aryanti, R. Yustiana, R.E.D. Purnama, I.G. Wenten, Performance and characterization of PEG400 modified PVC ultrafiltration membrane, Membr. Water Treat. 6 (2015) 379-392. https://doi.org/10.12989/mwt.2015.6.5.379.

[34] R. Singh, Introduction to Membrane Technology, in: R. Singh (Ed.), Membrane Technology and Engineering for Water Purification, Butterworth-Heinemann, 2015, pp. 1-80. https://doi.org/10.1016/B978-0-444-63362-0.00001-X.

[35] K. Kimura, Y. Hane, Y. Watanabe, G. Amy, N. Ohkuma, Irreversible membrane fouling during ultrafiltration of surface water, Water Res. 38 (2004) 3431-3441. https://doi.org/10.1016/j.watres.2004.05.007.

[36] S.E. Exley, L.C. Paslay, G.S. Sahukhal, B.A. Abel, T.D. Brown, C.L. McCormick, S. Heinhorst, V. Koul, V. Choudhary, M.O. Elasri, S.E. Morgan, Antimicrobial peptide mimicking primary amine and guanidine containing methacrylamide copolymers prepared by raft polymerization, Biomacromolecules 16 (2015) 3845-3852. https://doi.org/10.1021/acs.biomac.5b01162.

[37] A.F. Martins, S.P. Facchi, H.D.M. Follmann, A.G.B. Pereira, A.F. Rubira, E.C. Muniz, Antimicrobial activity of chitosan derivatives containing N-quaternized moieties in its backbone: a review, Int. J. Mol. Sci. 15 (2014) 20800-20832. https://doi.org/10.3390/ijms151120800.

[38] N. Malanovic, K. Lohner, Antimicrobial peptides targeting gram-positive bacteria, Pharmaceuticals 9 (2016) 59. https://doi.org/10.3390/ph9030059.

[39] Y.F. Yang, H.Q. Hu, Y. Li, L.S. Wan, Z.K. Xu, Membrane surface with antibacterial property by grafting polycation, J. Membr. Sci. 376 (2011) 132-141. https://doi.org/10.1016/j.memsci.2011.04.012.

[40] L. Timofeeva, N. Kleshcheva, Antimicrobial polymers: Mechanism of action, factors of activity, and applications, Appl. Microbiol. Biotechnol. 89 (2010) 475-92. https://doi.org/10.1007/s00253-010-2920-9.

[41] M.C. Giano, Z. Ibrahim, S.H. Medina, K.A. Sarhane, J.M. Christensen, Y. Yamada, G. Brandacher, J.P. Schneider, Injectable bioadhesive hydrogels with innate antibacterial properties, Nat. Commun. 5 (2014) 4095. https://doi.org/10.1038/ncomms5095.

[42] L. Goetz, B. Jalvo, R. Rosal, A.P. Mathew, Superhydrophilic anti-fouling electrospun cellulose acetate membranes coated with chitin nanocrystals for water filtration, J. Membr. Sci. 510 (2016) 238-248. https://doi.org/10.1016/j.memsci.2016.02.069.

[43] M.M. Azevedo, P. Ramalho, A.P. Silva, R. Teixeira-Santos, C. Pina-Vaz, A.G. Rodrigues, Polyethyleneimine and polyethyleneimine-based nanoparticles: novel bacterial and yeast biofilm inhibitors, J. Med. Microbiol. 63 (2014) 1167-1173. https://doi.org/10.1099/jmm.0.069609-0.

[44] D.J. Phillips, J. Harrison, S.J. Richards, D.E. Mitchell, E. Tichauer, A.T.M. Hubbard, C. Guy, I. Hands-Portman, E. Fullam, M.I. Gibson, Evaluation of the antimicrobial zctivity of cationic polymers against Mycobacteria: Toward antitubercular macromolecules, Biomacromolecules 18 (2017) 1592-1599. https://doi.org/10.1021/acs.biomac.7b00210.

SUPPLEMENTARY MATERIAL

Poly(vinyl chloride)-hyperbranched polyamidoamine ultrafiltration membranes with antifouling and antibiofouling properties

Berta Díez[1], Arcadio Sotto[2,*], Antonio Martín[3], Jesús Arsuaga[3], Roberto Rosal[1,*]

[1] Department of Chemical Engineering, University of Alcalá, E-28871 Alcalá de Henares, Madrid, Spain
[2] Department of Science Education, Rey Juan Carlos University. Camino del Molino, Fuenlabrada. Madrid, Spain.
[3] School of Experimental Science and Technology, ESCET, Rey Juan Carlos University, E-28933 Móstoles, Madrid, Spain

Contents:

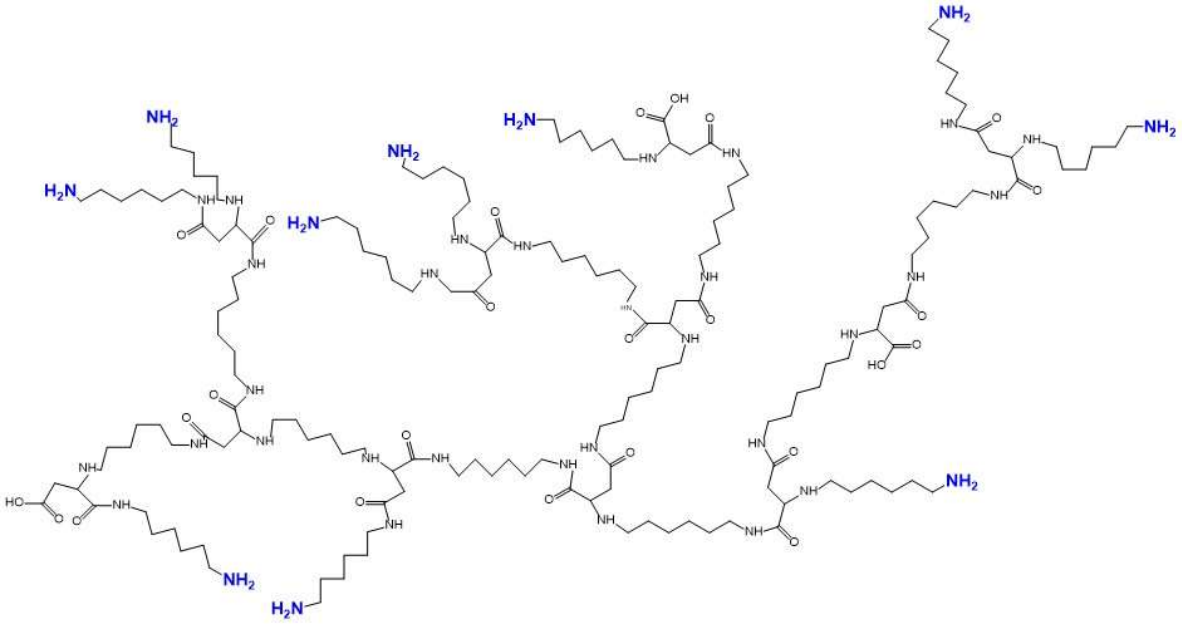

Figure S1. Chemical structure of Helux-3316. Primary amine end-groups (-NH_2) are shown in blue.

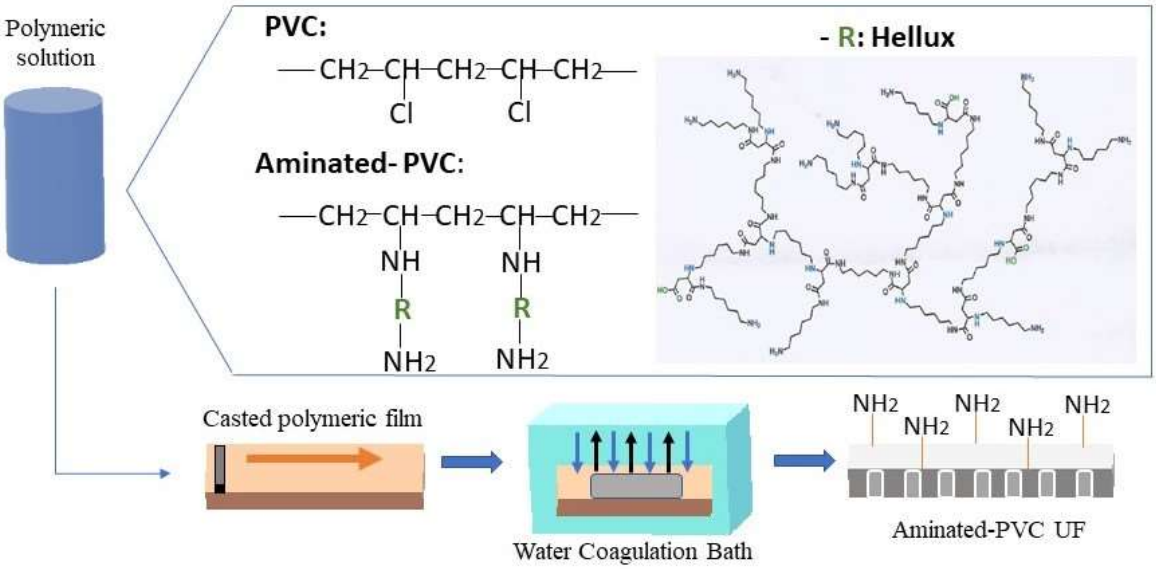

Figure S2. Schematic representation of the preparation of Helux-PVC ultrafiltration membranes.

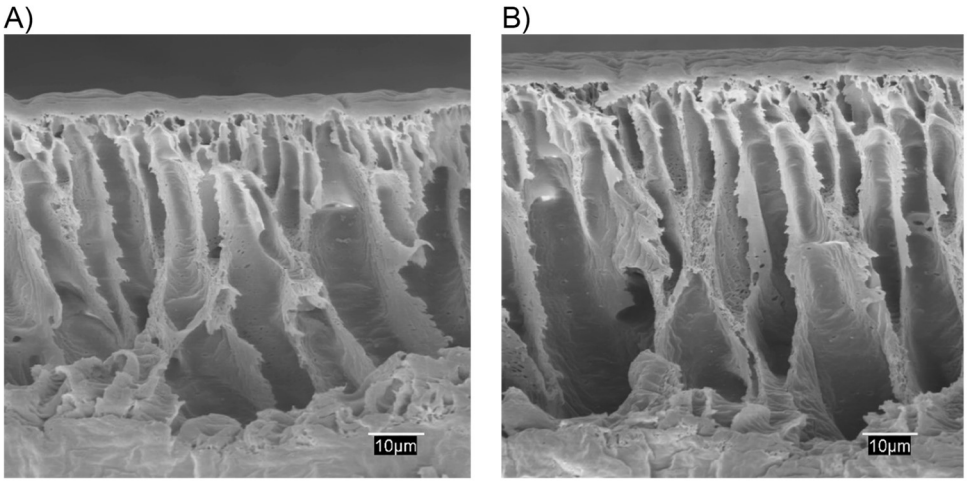

Figure S3. SEM cross-sectional images of PVC-H [0.8] (A) and PVC-H [1.6] (B) membranes.

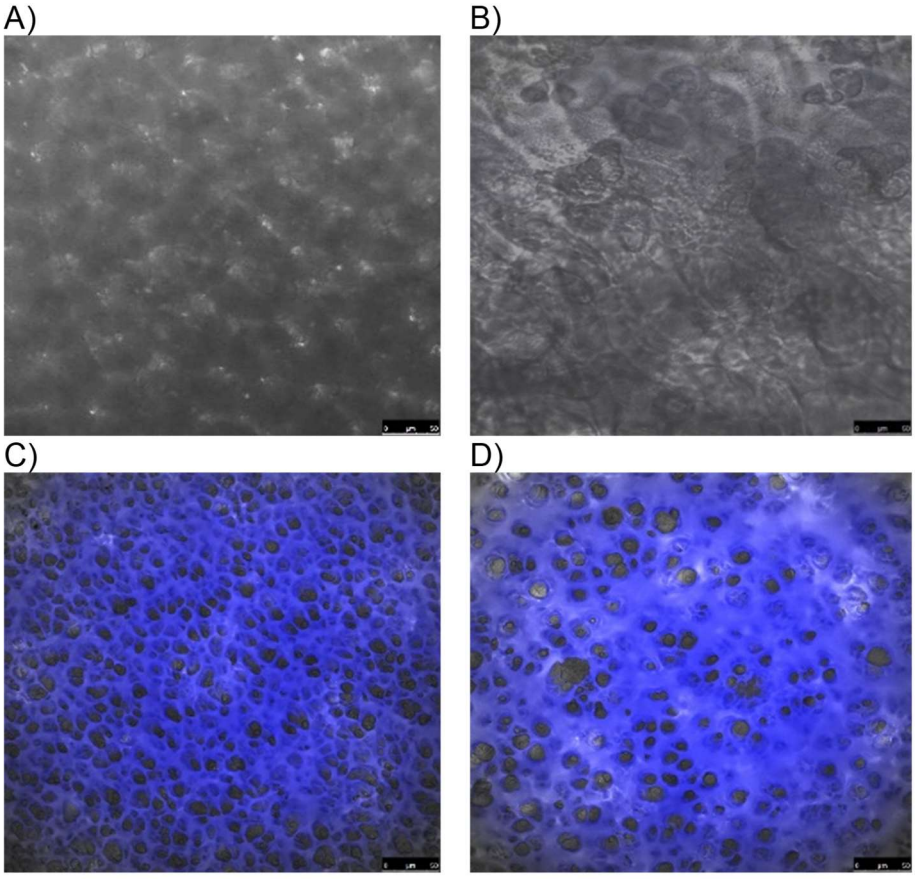

Figure S4. Confocal images of PVC (A), PVC-PVP (B), PVC-PVP-H [0.8] (C) and PVC-PVP-H [1.6] (D) membranes exposed to fluorescamine dye.

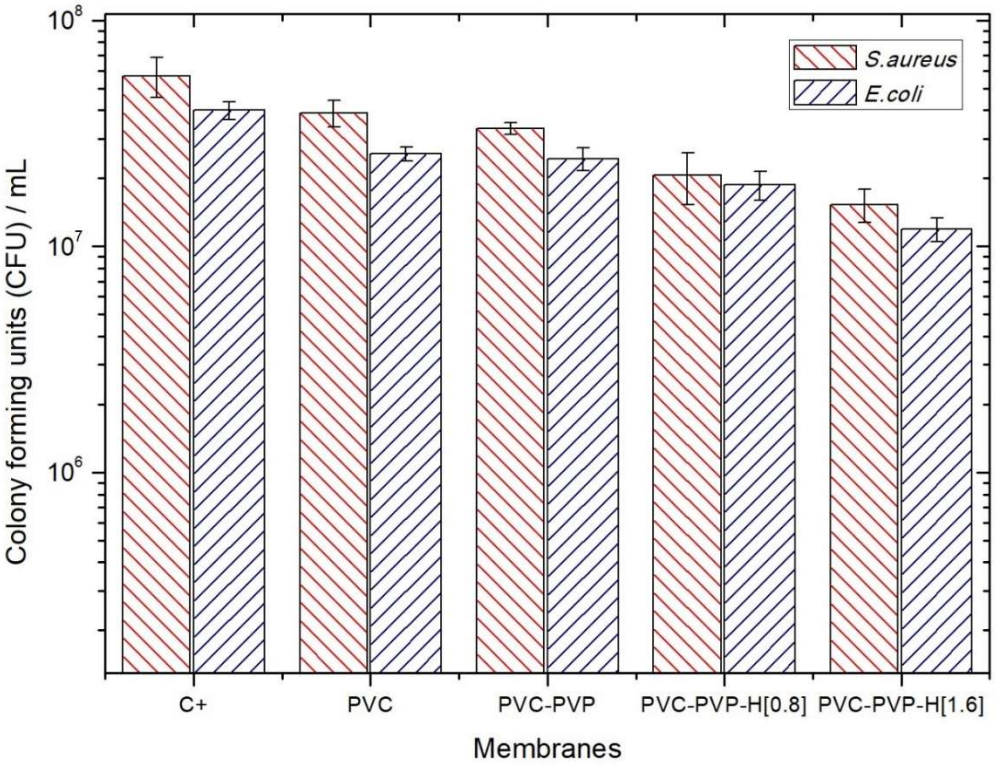

Figure S5. Microbial growth of *E.coli* (▨) and *S.aureus (▨)* cultures kept in contact with different membrane specimens at 36 ºC for 20 h.

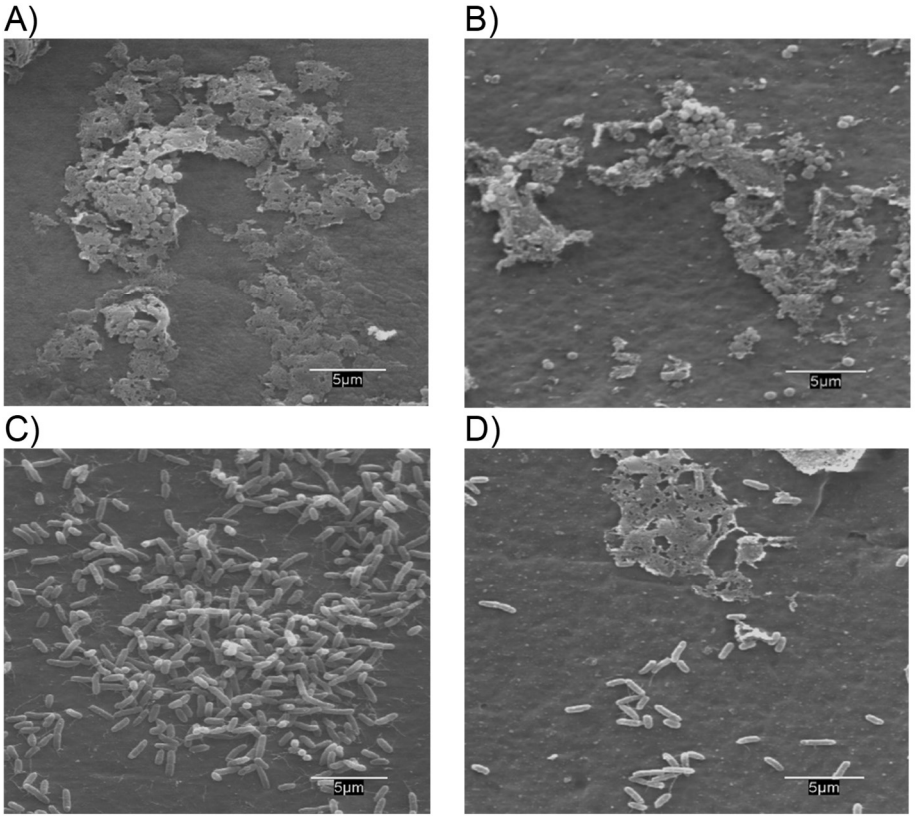

Figure S6. Microbial colonization of *S. aureus* (A-B) and *E. coli* (C-D) after maintaining bacterial cultures in contact for 20 h at 36 ºC with PVC-PVP (A-C) and PVC-PVP-H [0.8] membranes.